This article has been accepted for publication in a future issue of this journal, but has not been fully edited. Content may change prior to final publication. Citation information: DOI 10.1109/TIE.2015.2449780, IEEE Transactions on Industrial Electronics

Design and Optimisation of a Voice Coil Motor (VCM) with a Rotary Actuator for an Ultrasound Scanner

K.J. Smith, D.J. Graham and J.A. Neasham

***Abstract* —This paper proposes a new application for the rotary VCM. In developing a low cost ultrasound scanner for the developing world an oscillating transducer is required to sweep over the skin. The ultrasound scanner must operate from a USB power supply in remote locations. The application requires a 3.3N force on the coils of the motor to overcome the inertia of the skin. A proof of concept prototype motor with electronics has been designed, simulated and tested. The VCM optimisation is discussed in detail with the unique separation of the magnets being critical to reduce the axial bearing forces for this application.**

***Index Terms*—Voice Coil Motor (VCM), Rotary Actuator, Permanent Magnet (PM) Motor, 3D Finite-Element Analysis.**

I. Introduction

Ultrasound imaging is commonly used as a non-invasive diagnostic tool which employs either a linear, curved or 2D array of transducer elements [1] [2] [3]. Generally it is considered that the image quality and cost is proportional to the number of transducer elements [4]. As the number of elements increase so does the associated electronics which are required to transmit and receive on each element. The construction of multichannel phased array transducer would far exceed the target cost of this project. Thus a single transducer element design will be used which will require an actuator to create a synthetic array by mechanically moving the transducer. This method of combining a single transducer element and a mechanical actuator is unique in the context of modern medical ultrasound imaging [5] [6] [7] [8]. This is a compromise as the image quality is reduced but the cost saving is significant (over 95% cost reduction). Fig.1 shows a typical commercially available ultrasound probe compared to the prototype single element transducer.

Manuscript received December 8, 2014; revised April 28, 2015; accepted May 15, 2015.

K.J. Smith is with the School of Electrical and Electronic Engineering at Newcastle University, NE1 7RU (e-mail: kristopher.smith@ncl.ac.uk).

Fig.1: Comparison of the SonoSite Multichannel Array Transducer (left) [9] and the Prototype Single Element Ultrasound Scanner (right)

The process for controlling the ultrasound scanner is shown in Fig.2. The single transducer element is periodically activated at 0.25° increments over the scanning arm cycle. At each increment, a short pulse of 4.2MHz ultrasound is transmitted and the echo data is received, synthetically replicating a 200 element transducer array.

The low electrical noise of the PM rotary actuator Voice Coil Motor (VCM) is ideal for maintaining a high signal to noise ratio of the echo data and the accurate positional encoder allows the ultrasound image to be constructed at the end of each scanning cycle.

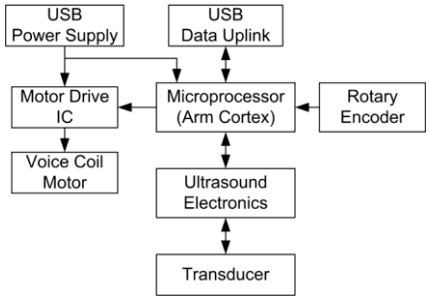

Fig.2: Ultrasound Scanner Hardware Control Process

The VCM rotary actuator shown in Fig.3 is commonly utilised in Hard Disk Drives (HDD) and optical storage devices i.e. the Blu-ray disc [10] [11]. The VCM is continually improved to reduce vibration [12], cope with the increase in volumetric density [13] and develop the control design for head positioning [14]. In recent years it is used for lens focusing and zooming on mobile camera phones due to the low current demands [15] [16]. The VCM is also applied to linear actuators which have wide applications in transportation and manufacturing [17] [18]. This paper describes a new application where the VCM is used to drive the swing arm of a portable low cost ultrasound scanner. The typical VCM of a HDD or optical storage device has a peak force of around 0.1N to sweep the head over the storage disc [10] [19]. The

This article has been accepted for publication in a future issue of this journal, but has not been fully edited. Content may change prior to final publication. Citation information: DOI 10.1109/TIE.2015.2449780, IEEE Transactions on Industrial Electronics

design challenge of the ultrasound scanner requires a force profile which is 33 times large in magnitude compared to the standard VCM design. The ultrasound scanner will have a strict USB 5V 500mA power supply with the VCM current limited to 300mA, given that 200mA is required for electronic control and periodic ultrasound data acquisition.

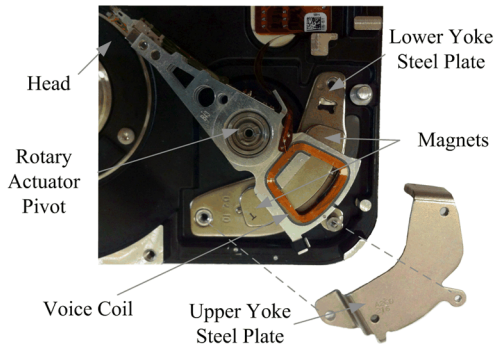

Fig.3: Configuration of a computer HDD with VCM

The VCM rotary actuator is directly coupled to the load, with no gears, cogs or brushes. This increases the motor life expectancy due to the limited number of moving parts and offers a high reliability [10] [20]. The VCM controlled swing arm will operate at 2Hz which will have low acoustic noise (compared to a geared system) but more importantly low electrical noise and simple control. The use of Permanent Magnet (PM) materials ensure a high torque density to current ratio [21] [22]. However, rare earth materials have the problem of high cost and limited supply [23].

The most common topology of the VCM for optical disc drives is shown in Fig.4 [24] [25]. The magnets are located on a single side, where the magnet placement creates flux leakage in the air gap which can cause an unwanted axial force.

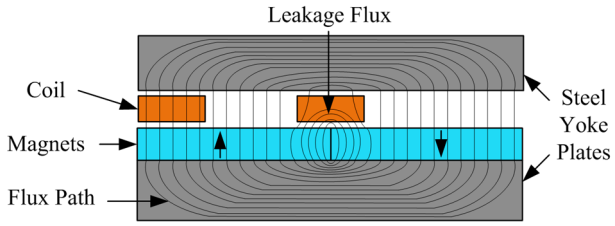

Fig.4: 2D Conventional Single Sided VCM

In Fig.5 an adaption of the Halbach [26] [27] magnetic circuit for the rotary VCMs was introduced by Sung-Q Lee et al [28]. The Halbach approach was applied by Y. Choi et al [29] to a HDD. It found for the same magnetic circuit volume (compared to a conventional VCM) the dynamic force increased by 11% but utilized 33% more magnet (due to the reduction in yoke flux saturation), thus improving the air gap flux density for a limited magnetic circuit volume. It also showed that when using the same magnet mass for both conventional and Halbach designs it offers little performance difference [29]. However the Halbach will have an increased manufacturing complexity and associated cost.

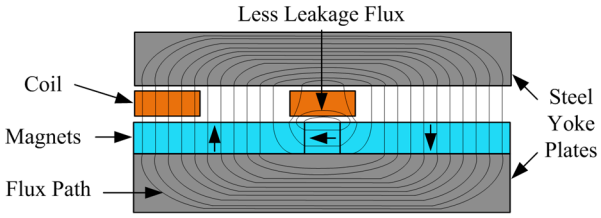

Fig.5: 2D Halbach Approach Single Sided VCM

The VCM operation is based on the Lorentz Force principle, where by driving a current through the voice coil placed in a PM field, a force will act upon the voice coil. If the voice coil is perpendicular to the PM field it can be seen that:

$$F = I\beta LN \qquad (1)$$

Where the resultant force (F) on the coil is proportional to the current (I), magnetic flux density (β), coil length (L) and the number of turns (N) within the PM field. In the conventional and Halbach VCM designs as the current carrying wire is moved above the magnet intersection, the force imposed by the leakage flux produces an unwanted axial force on the bearings, pushing the coil towards the steel yoke. Thus part of the magnet and magnetic field is wasted. This axial force has the potential to distort the path taken by the transducer as it sweeps. Any axial deflection will result in image distortion because it is assumed that each data acquisition point lies perfectly on a 2D arc. Fig.6 shows the new topology VCM to reduce this axial force whereby separating the magnets to achieve less leakage flux.

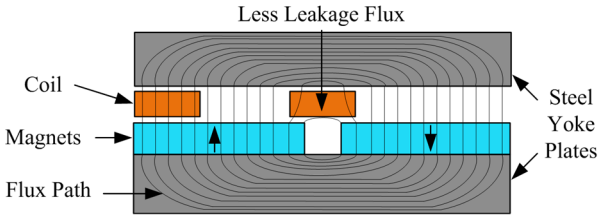

Fig.6: 2D Separated Magnet Single Sided VCM

II. DESIGN OF VCM ROTARY ACTUATOR

The application of using the VCM within the swing arm of an ultrasound scanner requires a sufficient force to overcome the inertia of the scanning head moving across the skin in a layer of coupling gel. From experimental results by attaching the ultrasound scanning head to a Sauter Digital Force Gauge FK50 it was ascertained that a peak 1.5N force is required at the scanning arm tip. The design of the casing limits the VCM position to be half the distance from the actuator pivot point to that of the scanning head. Thus the VCM will need to generated a peak 3.3N force acting on the coils (this includes a 10% margin of safety into the force requirement).

Fig.7 shows the ultrasound casing which is designed to limit the actuator swing arm to a range of 50 degrees. The voice coil

This article has been accepted for publication in a future issue of this journal, but has not been fully edited. Content may change prior to final publication. Citation information: DOI 10.1109/TIE.2015.2449780, IEEE Transactions on Industrial Electronics

size is limited to fit inside the coil support mount ensuring a maximum size of L50 x W30 mm.

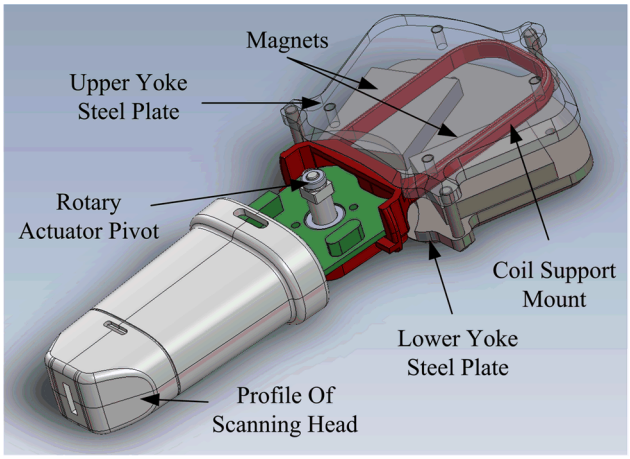

Fig.7: Ultrasound Scanner CAD Housing

The USB operated ultrasound limits the power available for the VCM to 1.5W (5V at 300mA) to allow normal device operation. Thus the voice coil resistance is ideally designed at 16.6Ω to achieve simple current limiting. Using the Lorentz principle (1) the following voice coil forces can be calculated in TABLE 1.

TABLE 1
VOICE COIL DESIGN

Model	Turns	Coil Area (mm^2)	Standard Wire OD (mm)	Coil Resistance (Ω)	Lorentz Force (N)
1	200	10	0.18	16.4	1.8
2	300	23	0.224	16.0	2.7
3	320	25.2	0.224	16.6	2.9
4	340	26.9	0.224	17.6	3.1
5	340	33.3	0.25	14.2	3.1
6	360	35.3	0.25	15.1	3.2
7	380	37.2	0.25	15.9	3.4
8	400	40	0.25	16.4	3.6

Thus the VCM design that satisfies the 3.3N peak force requirement is Model 7 (seen in TABLE 1), which has 380 turns, requiring a coil area of 37.2mm^2 assuming a 50% fill factor.

III. FINITE-ELEMENT SIMULATION AND ANALYSIS

The Infolytica MagNet (version 7.4) 3D Finite-Element (FE) simulation package is used to determine the magnetic field distribution for the VCM. Fig.8 and Fig.9 show the proposed structure of the actuator.

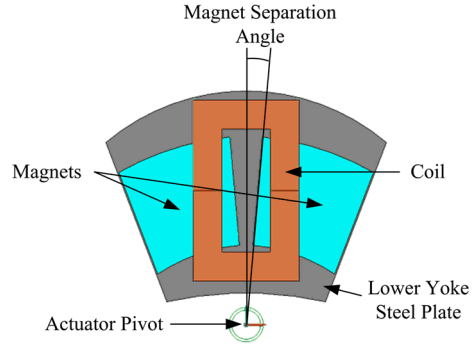

Fig.8: VCM Top View (Upper Yoke Removed)

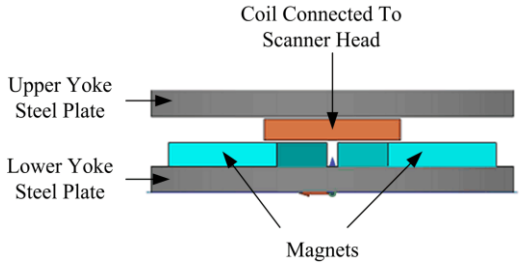

Fig.9: VCM Side View

To design the optimal VCM for this application the coil parameters have been calculated using the Lorentz force (TABLE 1) and designed based on the geometric case limits. The magnet size and position are optimised through the 3D FE parametric variation analysis. The yoke steel plates completing the electromagnet circuit are restricted to 8mm thick to avoid high flux saturation and reduced torque capability during the optimisation process [30] [31], though practically they need to be as thin as possible for practical device weight savings. A summary of the optimisation parameters is shown in TABLE 2.

TABLE 2
VCM PARAMETER RANGE

Symbol	Machine Parameters	Value	Units
MH	Magnet Height	1,2,3,4,5,6,7,8,9,10	mm
MS	Angle of Magnet Separation	0,2.5,5,7.5,10,12.5,15	degrees
IRE	Magnet Inner Radius Extension	0,1,2,3,4,5,6,7,8,9,10	mm
ORE	Magnet Outer Radius Extension	01,2,3,4,5,6,7,8,9,10	mm
cl	Coil Length	50	mm
c	Coil Inner Length	34	mm
cw	Coil Width	30	mm
ct	Coil Winding Thickness	8	mm
ml	Magnet Length	30	mm
	Lower Yoke Height	8	mm
	Upper Yoke Height	8	mm
	Air Gap	0.5	mm

Fig.10 identifies the motor design parameters outlined in TABLE 2.

This article has been accepted for publication in a future issue of this journal, but has not been fully edited. Content may change prior to final publication. Citation information: DOI 10.1109/TIE.2015.2449780, IEEE Transactions on Industrial Electronics

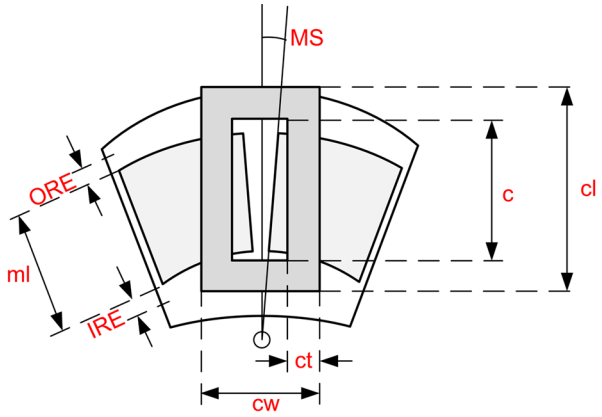

Fig.10: VCM Parameters and Structure

IV. OPTIMISATION PROCESS AND ANALYSIS

Through a variable matrix controller the design parameters are changed. The optimisation will be assessed by an objective function to identify the best design. The objective function is the maximisation of the scanning arm force with the minimisation of bearing axial force while using the smallest amount of magnet to satisfy the 3.3N scanner requirement. This can be represented as:

$$f_{OBJECTIVE} = \max\left\{\frac{Force_{PEAK\ \ SCANNER} - Force_{PEAK\ \ AXIAL}}{Magnet\ Mass}\right\} \quad (2)$$

With,

$$Force_{PEAK\ \ SCANNER} >= 3.3$$

As the Magnet Height (MH) increases and Angle of Magnet Separation (MS) decreases the total magnet mass used is increased, thus increasing the air gap flux density which in turn causes the peak force applied to the scanning head and the axial force applied to the bearing to increase.

Analysing Fig.11 the objective function identifies the optimal design with a magnet height of 5mm and a 10^{o} magnet separation angle, which uses 55g of Neodymium magnet. The graphical trend also confirms that during the optimisation process as the angle of magnet separation (MS) increases the axial force imposed on the bearings decreases due to the leakage flux reduction. This is highlighted in Fig.12 which shows the flux path for a conventional and Separated Magnet VCM with the same magnet mass. The flux leakage above the magnet intersection is 0.7T and 0.1T respectively. Thus changing the design to separate the magnets reduces the axial force on the bearing to allow a smooth scanning motion, while increasing the bearings life expectancy.

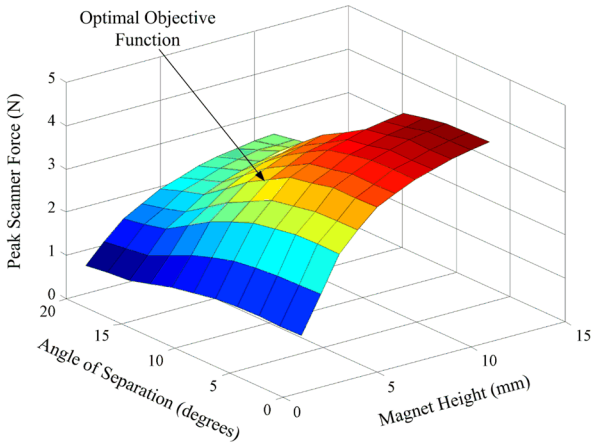

(a)

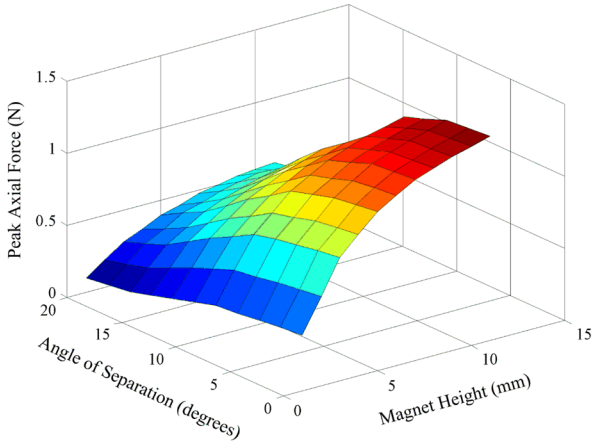

(b)

Fig.11: 3D FEA Parameter Optimisation Results for MS and MH (a) Peak Scanning Force (b) Peak Axial Force

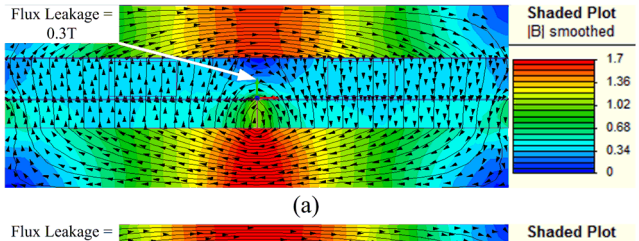

(a)

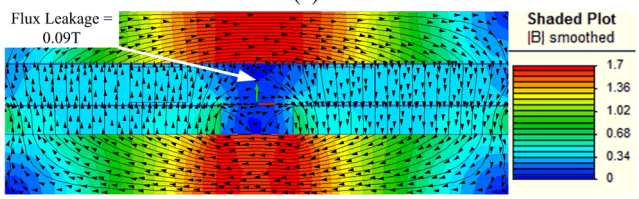

(b)

Fig.12: 2D Flux Path of (a) Conventional VCM (b) Separated Magnet VCM

The placement of the magnet relative to the coil design has a significant effect on the rotary arm and axial forces. Fig.10 has shown the magnet inner and outer radius edges fall 2mm (c-ml) away from the coil inner edges during the MS and MH optimisation. As the magnet edges outer radius (ORE) and inner radius (IRE) are extended they will fall directly under the top and bottom sections of the coil. The resultant effect of the magnet extension is shown in Fig.13. The results identify

This article has been accepted for publication in a future issue of this journal, but has not been fully edited. Content may change prior to final publication. Citation information: DOI 10.1109/TIE.2015.2449780, IEEE Transactions on Industrial Electronics

that as the ORE and IRE are extended the best case Scanning Head Force increases by 11%, while the worst case Axial Bearing Force increases by 43%.

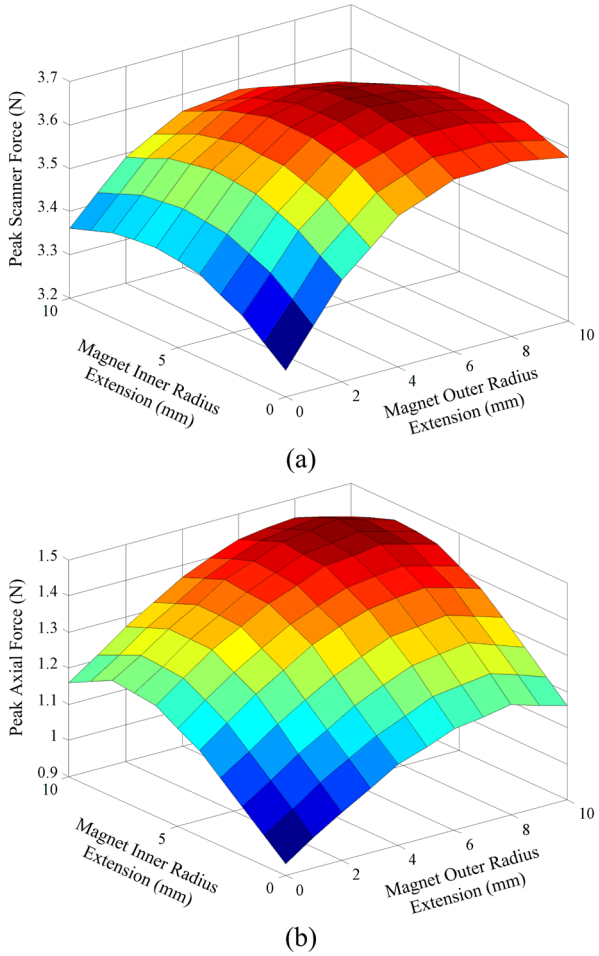

Fig.13: 3D FEA Parameter Optimisation Results for IRE and ORE (a) Peak Scanning Force (b) Peak Axial Force

V. SIMULATED FINAL OPTIMISED DESIGN FOR PRACTICAL IMPLEMENTATION

For fabrication a rectangular magnet is used to replace the arc magnet discussed in the optimisation process. This allows off the shelf magnets to be purchased reducing prototyping time and costs. Thus, the experimental results in Section VI. are compared to an updated FE model. Fig.14 shows a comparison of the Arc magnet and Rectangular magnet (L30 x W25 x H5 mm) over a complete mechanical scanner cycle. The peak and mean force changes by less than 3% for the scanning and axial forces. Thus the rectangular magnet is considered a suitable replacement to achieve the required motor performance.

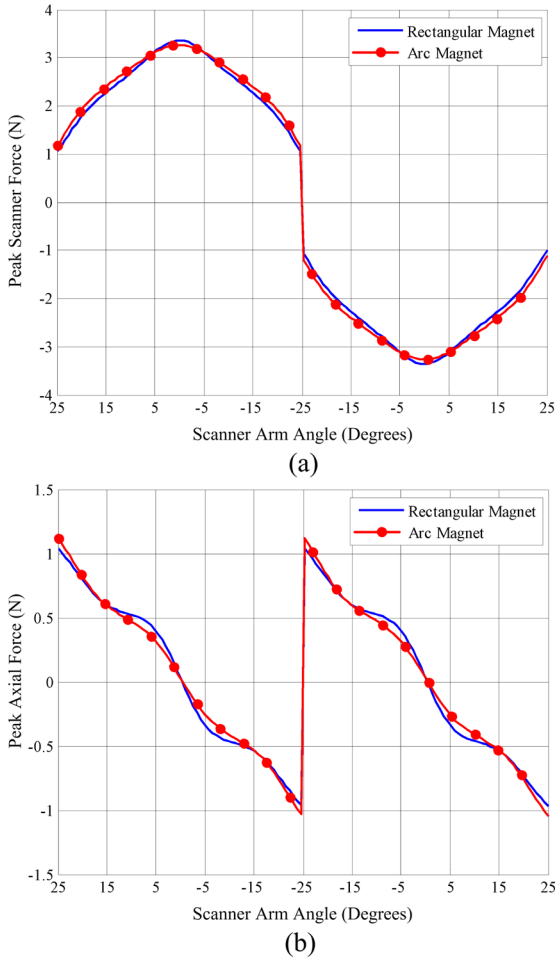

Fig.14: 3D FEA Comparison of Arc and Rectangular Magnets (a) Scanning Force (b) Axial Force

VI. FABRICATION AND EXPERIMENTAL RESULTS

After the VCM optimisation a prototype machine, as shown in Fig.15, is built for experimental validation. The motor is driven by a 5V USB power supply. The force measurements are taken using the Sauter Digital Force Gauge FK50.

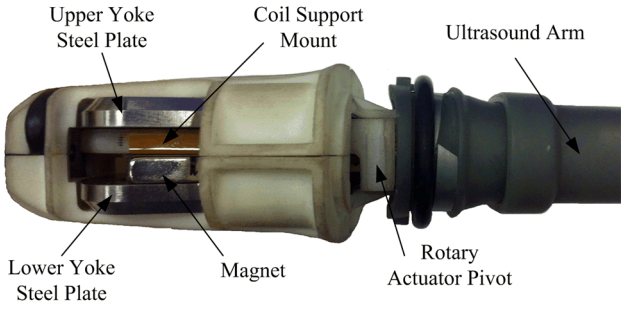

Fig.15: Prototype VCM machine design for the Ultrasound Scanner

The results for the simulated and experimental machine testing are shown in Fig.16. The axial forces couldn't be measured as the force is reduced so that the pivot bearings limiting any axial motion. The experimental results for the scanning force

This article has been accepted for publication in a future issue of this journal, but has not been fully edited. Content may change prior to final publication. Citation information: DOI 10.1109/TIE.2015.2449780, IEEE Transactions on Industrial Electronics

are within 10% of the estimated 3D FEA simulation. Using a Gauss Meter Probe the experimental machine yields a 10% higher air gap flux density than that of the simulated model. Thus taking into account manufacturing tolerance of magnets, air gaps and the housing construction this shows a good correlation between experimental and simulation results.

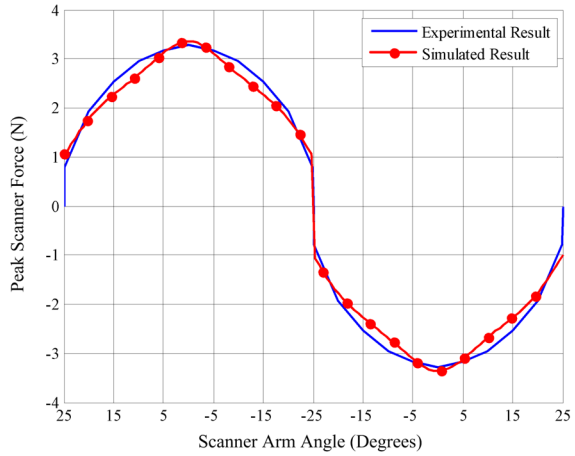

Fig.16: Comparing VCM experimental and 3D FEA simulation results of the Scanning Force

VII. CONCLUSIONS

A new magnet topology VCM rotary actuator has been designed and experimentally verified for the ultrasound scanner application. The experimental results are in good agreement with the predicted 3D FEA simulation, confirming the suitability of the motor for this application.

The VCM optimisation covers the unique magnet placement and angle of separation required to reduce the axial bearing forces. The simulation results show that by separating the magnets the air gap leaking flux density has dropped by 85% from 0.7T to 0.1T. This reduces the axial force and limits any deviation from the desired transducer movement arc which would result in image distortion.

The cost of the VCM motor components and drive electronics for the prototype machine is approximately $11, with the magnets accounting for nearly 70% of the total cost. Future work involves analysing a double sided VCM for a flatter force profile and simultaneously changing the magnet material to ferrite to see if the same performance can be achieve at an even cheaper cost.

ACKNOWLEDGMENTS

We should acknowledge EPSRC, via the Impact Acceleration Account, and Delft Imaging Systems for supporting this project.

REFERENCES

[1] G. Matrone, F. Quaglia, and G. Magenes, "Modeling and simulation of ultrasound fields generated by 2D phased array transducers for medical applications," in *Engineering in Medicine and Biology Society (EMBC), 2010 Annual International Conference of the IEEE*, 2010, pp. 6003-6006.

[2] A. Fenster, G. Parraga, and J. Bax, *Three-dimensional ultrasound scanning* vol. 1. Interface Focus - The Royal Society, 2011.

[3] R. W. Prager, U. Z. Ijaz, A. H. Gee, and G. M. Treece, "Three-dimensional ultrasound imaging," *Proceedings of the Institution of Mechanical Engineers, Part H: Journal of Engineering in Medicine,* vol. 224, pp. 193-223, February 1, 2010 2010.

[4] F. Aaron, B. D. Dónal, and H. N. Cardinal, "Three-dimensional ultrasound imaging," *Physics in Medicine and Biology,* vol. 46, p. R67, 2001.

[5] J. Neasham and D. Graham, "Ultrasound imaging apparatus," *UK Patent Application GB 2515601,* Application No.1404266.7, Dec. 2014.

[6] J. Neasham and D. Graham, "Ultrasound imaging apparatus," *US Patent Application,* Application No. US201313974483 20130823, Sept. 2014.

[7] J. Neasham and D. Graham, "Ultrasound imaging apparatus," *World Intellectual Property Organization Patent,* Application No.WO2014140557, Sept. 2014.

[8] A. Gee, R. Prager, G. Treece, and L. Berman, "Engineering a freehand 3D ultrasound system," *Pattern Recognition Letters,* vol. 24, pp. 757-777, 2003.

[9] "SonoSite Ultrasound Transducer C60N," *http://www.sonosite.com/*.

[10] D.-J. Lee, J.-S. Oh, S.-U. Kim, J.-H. Yoo, N.-C. Park, Y.-P. Park, T. Shimano, and S. Nakamura, "Design of swing arm actuator for small and slim optical disc drives," *Microsystem Technologies,* vol. 13, pp. 1307-1313, 2007/05/01 2007.

[11] E. J. Hong, D. W. Kim, N. C. Park, H. S. Yang, Y. P. Park, and S. K. Kim, "Design of swing arm type actuator and suspension for micro optical disk drive," *Microsystem Technologies,* vol. 11, pp. 1085-1093, 2005/08/01 2005.

[12] T. Atsumi, A. Okuyama, and S. Nakagawa, "Vibration Control Above the Nyquist Frequency in Hard Disk Drives," *IEEE Trans. Ind. Electron.,* vol. 55, pp. 3751-3757, 2008.

[13] K. Thongpull, N. Jindapetch, and W. Teerapabkajorndet, "Wireless ESD Event Locator Systems in Hard Disk Drive Manufacturing Environments," *IEEE Trans. Ind. Electron.,* vol. 60, pp. 5252-5259, 2013.

[14] T. Atsumi and W. C. Messner, "Optimization of Head-Positioning Control in a Hard Disk Drive Using the RBode Plot," *IEEE Trans. Ind. Electron.,* vol. 59, pp. 521-529, 2012.

[15] K.-H. Kim, S.-Y. Lee, and S. Kim, "A mobile auto-focus actuator based on a rotary VCM with the zero holding current," *Optics Express,* vol. 17, pp. 5891-5896, 2009/03/30 2009.

[16] C.-S. Liu and P. D. Lin, "A miniaturized low-power VCM actuator for auto-focusing applications," *Optics Express,* vol. 16, pp. 2533-2540, 2008/02/18 2008.

[17] Y. Liang, Z. Lei, J. Zongxia, H. Hongjie, C. Chin-Yin, and I. M. Chen, "Armature Reaction Field and Inductance of Coreless Moving-Coil Tubular Linear Machine," *IEEE Trans. Ind. Electron.,* vol. 61, pp. 6956-6965, 2014.

[18] P. E. Kakosimos, A. G. Sarigiannidis, M. E. Beniakar, A. G. Kladas, and C. Gerada, "Induction Motors Versus Permanent-Magnet Actuators for Aerospace Applications," *IEEE Trans. Ind. Electron.,* vol. 61, pp. 4315-4325, 2014.

[19] L. Dong-Ju, W. Ki-Suk, N.-C. Park, and P. Young-Pil, "Design and optimization of a linear actuator for subminiature optical storage devices," *IEEE Trans. Magn.,* vol. 41, pp. 1055-1057, 2005.

[20] A. Tenconi, S. Vaschetto, and A. Vigliani, "Electrical Machines for High-Speed Applications: Design Considerations and Tradeoffs," *IEEE Trans. Ind. Electron.,* vol. 61, pp. 3022-3029, 2014.

[21] C. Ming, H. Wei, Z. Jianzhong, and Z. Wenxiang, "Overview of Stator-Permanent Magnet Brushless Machines," *IEEE Trans. Ind. Electron.,* vol. 58, pp. 5087-5101, 2011.

[22] I. Petrov and J. Pyrhonen, "Performance of Low-Cost Permanent Magnet Material in PM Synchronous Machines," *IEEE Trans. Ind. Electron.,* vol. 60, pp. 2131-2138, 2013.

[23] Z. Wenliang, T. A. Lipo, and K. Byung-il, "Material-Efficient Permanent-Magnet Shape for Torque Pulsation Minimization in SPM Motors for Automotive Applications," *IEEE Trans. Ind. Electron.,* vol. 61, pp. 5779-5787, 2014.

[24] L. Dong-Ju, W. Jung-Hyun, K. Sa-Ung, O. Je-Seung, Y. Jeong-Hoon, P. No-Cheol, P. Young-Pil, S. Takeshi, and N. Shigeo,

"Development of “L-Shaped” Rotary Voice Coil Motor Actuator for Ultra Slim Optical Disk Drive Using Integrated Design Method based on Coupled-Field Analysis," *Japanese Journal of Applied Physics,* vol. 46, p. 3715, 2007.

[25] L. Huai, L. Qinghua, H. Zhimin, and C. Shixin, "Development of a single coil coupled force VCM actuator for high TPI magnetic recording," *IEEE Trans. Magn.,* vol. 37, pp. 850-854, 2001.

[26] D. A. Young-Man Choi, Dae-Gab Gweon, and Jaehwa Jeong, "K. Halbach, “Design of permanent multi pole magnets with oriented area earth cobalt material” " *Journal of Magnetics,* vol. 169, pp. 1-10, 1980.

[27] S. Dwari and L. Parsa, "Design of Halbach-Array-Based Permanent-Magnet Motors With High Acceleration," *IEEE Trans. Ind. Electron.,* vol. 58, pp. 3768-3775, 2011.

[28] Q. L. Sung, P. Kang-Ho, P. Mun-Cheal, and K. Kwang-Yong, "Halbach-Magnet-Array-Based Focusing Actuator for Small-Form-Factor Optical Storage Device," *Japanese Journal of Applied Physics,* vol. 45, p. 1131, 2006.

[29] "Y. Choi, D. Ahn, D. Gweon, and J. Jeong, "Halbach magnetic circuit for voice coil motor in hard disk drives," *Journal of Magnetics*, vol. 15, no. 3, pp. 143-147, 2010.."

[30] K. I. Laskaris and A. G. Kladas, "Permanent-Magnet Shape Optimization Effects on Synchronous Motor Performance," *IEEE Trans. Ind. Electron.,* vol. 58, pp. 3776-3783, 2011.

[31] K. I. Laskaris and A. G. Kladas, "Internal Permanent Magnet Motor Design for Electric Vehicle Drive," *IEEE Trans. Ind. Electron.,* vol. 57, pp. 138-145, 2010.

Kristopher J. Smith completed an apprenticeship with British Telecom before attended Northumbria University. Here he received a BSc(Hons) in Communications & Electronic Engineering and a MSc in Microelectronic Engineering. In 2006 he joined Newcastle University to complete an Engineering Doctorate (EngD) with sponsorship from Dyson. His research focused on Power Supply Quality in Brushless Drives. After completing the doctorate Kris has moved into a Teaching Fellowship at Newcastle University. His research interests are mainly in permanent magnet machine design.

David J. Graham received the B.Eng degree in electronic engineering and the Ph.D degree in electronic communications from Newcastle University, Newcastle upon Tyne, U.K. in 2007 and 2011 respectively. His Ph.D study focussed on through metal communications and power delivery.

Since graduating he has worked as Research Associate in the Communications, Sensors, Signal & Information Processing Research Group (ComS2IP) at Newcastle University. His research interests include acoustic communication, digital signal processing, wireless sensor networks and medical imaging.

Jeffrey A. Neasham received the B.S. degree in electronic engineering from Newcastle University, UK, in 1994. He then worked there until 2007 as a Research Associate on research and commercial product development in underwater acoustic communication, sonar imaging, and wireless sensor networks, before taking up an academic post. He is currently a Senior Lecturer in communications and signal processing with the School of Electrical and Electronic Engineering, Newcastle University.